

An analytical model for the determination of stability boundaries in a natural circulation single-phase thermosyphon loop

M. Maiani ^a, W.J.M. de Kruijf ^a, W. Ambrosini ^{b,*}

^a *Interfaculty Reactor Institute, Delft University of Technology, Mekelweg 15, 2629 JB Delft, The Netherlands*

^b *Dipartimento di Ingegneria Meccanica, Nucleare e della Produzione, Università di Pisa, via Diotisalvi 2, 56126 Pisa, Italy*

Received 18 May 2002; accepted 26 July 2003

Abstract

In this paper, an extension of previous analyses of natural circulation in a simple single-phase loop is presented. Assuming more general correlations for the friction factor and the heat transfer coefficient, an analytical model describing the system is obtained and a parametric representation of its dynamic behaviour is achieved. On this basis, stability maps can be drawn. A preliminary validation of the analytical model has been carried out by using an independent program developed for the analysis of stability in natural circulation loops. The aim of the present work is to provide a simple analytical tool devoted to the stability analysis of a reference single-phase loop. This model can be applied in a relatively wide range of conditions and regimes to provide benchmark solutions for thermal-hydraulic codes and related nodalisations.

© 2003 Elsevier Inc. All rights reserved.

Keywords: Natural circulation; Stability; Thermosyphon loop

1. Introduction

In spite of their apparent simplicity, natural circulation thermosyphon loops appear to be very interesting systems from both the scientific and the technical points of view. In fact, they are well known examples of simple non-linear systems that can exhibit complex (i.e., chaotic) behaviour (see, e.g., Bau and Wang, 1992; Hilborn, 2000). Furthermore, natural circulation is extensively applied in industry and, in particular, in nuclear reactors: in this case, natural circulation is one of the fundamental physical mechanisms that the safe operation of innovative nuclear power plants relies upon. Typically, passive heat removal during normal operation or during postulated accident conditions is ensured by natural circulation. This makes its study and the assessment of the related system codes interesting topics for both PWR ¹ and BWR ² systems. Moreover, natural circu-

lation in the core, with no need for motor-driven circulation pumps, is one of the main features of the ESBWR ³ reactor (Challberg et al., 1998), currently under development.

In the past decades, natural circulation loops have been the subject of a considerable research effort, focused on their very interesting stability behaviour. Pioneering works in this field have been published by Welander (1965), who has identified the possibility of oscillating behaviour in natural circulation loops, and Keller (1966), who has suggested that, under particular conditions, oscillations could become periodic. In 1967, Welander published a further paper (Welander, 1967) in which he analysed the stability of a very schematic thermosyphon loop, consisting of two vertical adiabatic legs joined by two short heated and cooled sections. For some values of the friction and buoyancy parameters, growing instabilities were reported to occur, leading to repeated flow reversals. Experiments conducted in a toroidal loop by Creveling et al. (1975) have demonstrated that such a curious behaviour could

* Corresponding author. Tel.: +39-50-836673; fax: +39-50-836665.

E-mail address: walter.ambrosini@ing.unipi.it (W. Ambrosini).

¹ Pressurized water reactor.

² Boiling water reactor.

³ European simplified boiling water reactor.

Nomenclature

a, b, c	dimensionless constants for the friction factor law	Π_w	wetted perimeter [m]
A	channel flow area [m^2]	ρ	density [kg/m^3]
c_p	specific heat at constant pressure [$\text{J}/(\text{kg K})$]	ξ	heat transfer coefficient law parameter
D	pipe diameter [m]	τ	dimensionless time, $= \frac{t}{[L/(2k\Delta S)]}$
d	dimensionless exponent for the heat transfer coefficient law	θ	dimensionless temperature, $= \frac{T-T_0}{\Delta T}$
f	Darcy friction factor	$\bar{\theta}$	steady-state dimensionless temperature
g	local component along the pipe axis of the gravity acceleration [m/s^2]	$\delta\theta$	perturbation of the dimensionless temperature
H	heat transfer coefficient [$\text{W}/(\text{m}^2 \text{K})$]	θ_0	initial condition for the dimensionless temperature
\bar{H}	steady-state heat transfer coefficient [$\text{W}/(\text{m}^2 \text{K})$]	θ^+	steady-state dimensionless temperature in the ascending leg
L	closed loop total length [m]	θ^-	steady-state dimensionless temperature in the descending leg
$\frac{Q}{\bar{Q}}$	volumetric flow rate [m^3/s]	<i>Dimensionless groups</i>	
q	dimensionless volumetric flow rate	k	$\frac{\Pi_w \xi \bar{Q}^d}{A \rho c_p}$
\bar{q}	dimensionless steady-state volumetric flow rate	m	$\text{e}^{-\frac{1}{q}}$
q_0	initial condition for the dimensionless volumetric flow rate	n	$2(1-d) \text{e}^{-\frac{1}{q}} \left[\left(1 + \text{e}^{-\frac{1}{q}} \right) \bar{q}^2 \right]^{-1}$
δq	perturbation of the dimensionless volumetric flow rate	Re	Reynolds number, $\frac{\rho \bar{Q} D}{A \mu}$
S	curvilinear abscissa along the loop axis [m]	α	$\frac{g \beta L \Delta T}{2(k \Delta S)^2}$
s	dimensionless curvilinear abscissa along the loop axis	α^*	$\frac{g \beta L \Delta T}{2} \left[\frac{(\rho c_p)^{\frac{1}{(1-d)}} A}{(\Pi_w \xi \Delta S)^{\frac{1}{(1-d)}}} \right]^2$
ΔS	length of the heat source and sink horizontal pipes [m]	$\tilde{\alpha}$	$\frac{\pi n}{q}$
T	local cross-section averaged fluid temperature [K]	φ	$\frac{a \Pi_w L}{16 A} \left(\frac{\mu}{\rho D k \Delta S} \right)^b$
T_0	reference temperature [K], $= \frac{(T_w)_{\text{heater}} + (T_w)_{\text{cooler}}}{2}$	φ^*	$\frac{a \Pi_w L}{16 A^{1-b}} \left[\frac{\frac{1}{\mu c_p^{(1-d)}}}{\rho^{\frac{-d}{(1-d)}} D (\Pi_w \xi \Delta S)^{\frac{1}{(1-d)}}} \right]^b$
T_w	wall temperature [K]	γ	$\frac{\Pi_w c L}{16 A}$
$(T_w)_{\text{heater}}$	wall temperature in the heated section [K]	λ	$\frac{\gamma}{\alpha^*}$
$(T_w)_{\text{cooler}}$	wall temperature in the cooled section [K]	ν	$\left[\frac{\Pi_w \xi \Delta S}{\rho c_p \bar{Q}^{(1-d)}} \right]^d$
ΔT	reference temperature difference [K], $= \frac{(T_w)_{\text{heater}} - (T_w)_{\text{cooler}}}{2}$	σ	$\frac{\varphi^*}{\alpha^*}$
t	time [s]	Θ	$2\gamma \bar{q} + \varphi(2-b) \bar{q}^{(1-b)}$
<i>Greeks</i>		$\tilde{\Theta}$	$\frac{\Theta}{q}$
β	isobaric thermal expansion coefficient [K^{-1}]		
μ	dynamic viscosity [$\text{kg}/(\text{m s})$]		

actually occur in real life equipment. The subsequent work performed up to the present time has been devoted to both experimental and theoretical investigation of these aspects (see, e.g., Greif et al., 1979; Zvirin, 1979; Zvirin and Greif, 1979; Bau and Torrance, 1981; Hart, 1984, 1985; Chen, 1985; Sen et al., 1985; Misale and Tagliafico, 1987; Vijayan and Date, 1990, 1992; Velazquez, 1994; Venkat Raj, 1994; Vijayan and Austregesilo, 1994; Vijayan et al., 1995; Rodriguez-Bernal, 1995; Frogheri et al., 1997; Misale et al., 1999; Vijayan, 2002).

Part of the interesting information coming from this considerable body of literature is summarised hereafter.

Experiments have been mostly performed in simple configurations, mainly addressing rectangular loops. However, even more complex loops have been also considered, which may be closer to practical applications (see, e.g., Vijayan and Date, 1990, 1992; Venkat Raj, 1994). In addition, scaling laws for natural circulation phenomena have been proposed, giving the possibility to exploit the information on natural circulation

gathered from small scale facilities in predicting the behaviour of larger plants (see, e.g., Vijayan and Austregesilo, 1994; Vijayan, 2002).

The dynamic characteristics of thermosyphon loops have been also analysed by making use of mathematical models (see, e.g., Hart, 1984, 1985; Sen et al., 1985; Bau and Wang, 1992; Velazquez, 1994; Rodriguez-Bernal, 1995). Their behaviour turned out to be complex and strongly sensitive to the initial conditions, whatever the simplicity of the geometrical configuration is. In addition to Welander's loop, a striking example in this respect is the toroidal thermosyphon loop (Hart, 1984, 1985; Sen et al., 1985), whose dynamics, under appropriate boundary conditions, can be described by only three ordinary differential equations. Nevertheless, the predicted long term evolution of its relevant phase space variables is chaotic and closely related to the Lorenz attractor (Lorenz, 1963).

Analysis of natural circulation by space and time numerical discretisation of the governing equations is the only practical choice in complex cases as industrial plants, since their geometrical and functional details can hardly be represented using alternative techniques. Nevertheless, the application of large system codes to stability analyses must be considered with due caution, owing to the spurious numerical effects that discretisation brings about. This has been the subject of previous studies (Ambrosini and Ferreri, 1998, 2000; Ambrosini, 2001; Ambrosini et al., 2001) aimed at clearly identifying such effects in the stability maps of simple systems as predicted by codes and numerical methods in general. Needless to say, the role of the experiments carried out in full-scale or downscaled facilities cannot be substituted by any analytical procedure in the validation of thermal-hydraulic codes. However, the availability of benchmark problems that can be solved analytically gives some additional advantages in testing such codes on a wide range of geometric parameters and physical conditions.

In this perspective, the simple Welander's thermosyphon loop (Welander, 1967) turns out to be a very good reference example of single-phase natural circulation. As such, it has been taken as the basis for the mentioned studies on the prediction of stability by different numerical methods (see, e.g., Ambrosini and Ferreri, 1998; Ambrosini, 2001). Nevertheless, the assumptions originally adopted for the friction factor and for the heat transfer coefficient in Welander's paper (Welander, 1967) may be not general enough to allow a meaningful comparison between analytical and numerical predictions obtained by different codes. The restrictions imposed on the friction factor and on the heat transfer coefficient in Welander's paper, which have been partly removed in some recent developments (Ambrosini and Ferreri, 1998) can be further relaxed, reaching a higher level of generality. This allows obtaining more general

reference solutions for code validation and parametric studies.

The aim of this paper is to further extend Welander's treatment of the problem, including more flexible relationships for the friction factor and for the heat transfer coefficient as adopted in codes. According to the extended model, new stability maps are therefore obtained. Furthermore, the validation of the extended analytical model via a recently developed transient code (Ambrosini, 2001) is presented.

2. Description of the problem

A detailed description of the problem characteristics can be found in Welander (1967) and Ambrosini and Ferreri (1998). Briefly, looking at Fig. 1(a), the closed loop of total length L is made by two vertical adiabatic legs, joined at the top and at the bottom by two short horizontal pipes of length ΔS , where heat transfer is supposed to take place. In particular, heat transfer at controlled wall temperature is considered in top and bottom horizontal sections. If the wall temperature in the bottom section is higher than in the top one, a natural circulation regime can occur. In steady-state conditions, the fluid motion is governed by the balance of the opposite effects of buoyancy (due to the different fluid densities in the ascending—warm—and in the descending—cold—legs), and friction. The Boussinesq approximation for the fluid is used, i.e., the fluid is characterized by a positive thermal expansion coefficient β but it is still assumed to be incompressible (the density is insensitive to the weak pressure variations encountered in the problem).

In the original Welander's paper (Welander, 1967), a constant heat transfer coefficient is used in the heated

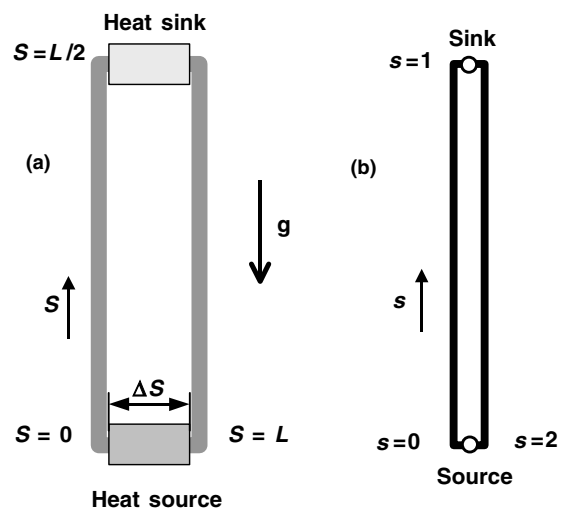


Fig. 1. Sketches of the considered physical system.

and cooled sections and a laminar flow friction factor is assumed; on the other hand, in the current treatment, the heat transfer coefficient and the friction factor are assumed to depend on the flow rate. The following models are considered for Darcy friction factor f and heat transfer coefficient H

$$f = c + \frac{a}{(Re)^b}, \quad (1)$$

$$H = \xi Q^d \quad (0 \leq d < 1), \quad (2)$$

where Re is the Reynolds number (based on the pipe diameter D), a, b, c, d, ξ are appropriate constants and Q is the volumetric flow rate. By choosing the appropriate values for d and ξ , correlation (2) gives the constant heat transfer coefficient case as well as the Colburn or the Dittus–Boelter correlations. In the two latter cases, it has to be noted that the coefficient ξ turns out to be dependent on the fluid temperature in the source and the sink.

For the loop represented in Fig. 1(a), the momentum equation takes the following form

$$\begin{aligned} \frac{dQ}{dt} + \frac{\Pi_w c}{8A^2} Q|Q| + \frac{\Pi_w a}{8A^{2-b}} \left(\frac{\mu}{\rho D} \right)^b Q|Q|^{1-b} \\ = \frac{\beta A}{L} \int_0^L g(S)(T - T_0) dS, \end{aligned} \quad (3)$$

where t is time, ρ and μ are the density and the dynamic viscosity, respectively, β is the isobaric thermal expansion coefficient, A is the channel flow area, S is the curvilinear abscissa along the loop axis, Π_w is the wetted perimeter, $g(S)$ is the local component along the pipe axis of the acceleration due to gravity. $T = T(S, t)$ is the local cross-section averaged fluid temperature and T_0 is a reference temperature for the problem defined by

$$T_0 = \frac{(T_w)_{\text{heater}} + (T_w)_{\text{cooler}}}{2}, \quad (4)$$

where $(T_w)_{\text{heater}}$ and $(T_w)_{\text{cooler}}$ are the wall temperatures (T_w) in the heated section (source) and in the cooled one (sink), respectively. T_0 can also be considered as a sort of average temperature at which all the fluid properties, in the present approximation, are calculated. It has a constant value as long as the wall temperatures T_w within heat source and sink are kept constant.

The energy equation, neglecting the production term due to friction and the pressure derivative term, takes the form

$$\begin{aligned} \frac{\partial T}{\partial t} + \frac{Q}{A} \frac{\partial T}{\partial S} \\ = \begin{cases} 0 & \text{in the legs,} \\ \frac{\Pi_w \xi Q^d}{A \rho c_p} (T_w - T) & \text{in the heater and the cooler} \end{cases} \end{aligned} \quad (5)$$

with $0 \leq S \leq L$, $t > 0$ and where c_p is the fluid specific heat at constant pressure.

On the basis of Eq. (2), the relation $\overline{H} = \xi \overline{Q}^d$ between steady-state heat transfer coefficient and volumetric flow must hold and the following quantity can be defined

$$k = \frac{\Pi_w \xi \overline{Q}^d}{A \rho c_p}. \quad (6)$$

In similarity with Welander's treatment, the following non-dimensional quantities are therefore introduced:

$$s = S \cdot \left(\frac{2}{L} \right), \quad (7a)$$

$$\tau = \frac{t}{[L/(2k \Delta S)]}, \quad (7b)$$

$$q = \frac{Q}{k A \Delta S}, \quad (7c)$$

$$\theta = \frac{T - T_0}{\Delta T}, \quad (7d)$$

where

$$\Delta T = \frac{(T_w)_{\text{heater}} - (T_w)_{\text{cooler}}}{2}. \quad (8)$$

It is worthwhile to remark that the factors used in relations (7b) and (7c) to make t and Q dimensionless both depend on the volumetric steady-state flow rate, whose value is, at the present stage, unknown. This is an important difference with respect to the original treatment by Welander, where all the quantities entering the corresponding factor are constant. Nevertheless, since these definitions are convenient, as it will become clear later on, we can presently consider \overline{Q} as an assigned (constant) quantity.

Moreover, again in similarity with Welander's treatment, we take the limit for $\Delta S \rightarrow 0$ (i.e., for vanishing sink and source length) while keeping constant the product $(\xi \Delta S)$.

Upon introduction of the above dimensionless quantities, it can be verified that the momentum equation (3) takes the form

$$\frac{dq}{d\tau} + \gamma q|q| + \varphi q|q|^{1-b} = \alpha \int_0^1 \theta ds, \quad (9)$$

while the energy equation (5) transforms into

$$\frac{\partial \theta}{\partial \tau} + q \frac{\partial \theta}{\partial s} = 0 \quad (0 < s < 1, \tau > 0), \quad (10)$$

where the following dimensionless parameters have been introduced

$$\gamma = \frac{\Pi_w c L}{16A} \quad (\text{not depending on } \overline{Q}), \quad (11a)$$

$$\varphi = \frac{a \Pi_w L}{16A} \left(\frac{\mu}{\rho D k \Delta S} \right)^b \quad (\text{depending on } \overline{Q}), \quad (11b)$$

$$\alpha = \frac{g\beta L \Delta T}{2(k \Delta S)^2} \quad (\text{depending on } \bar{Q}). \quad (11c)$$

To get Eqs. (9) and (10), the anti-symmetry of the temperature distribution along the loop has been taken into account (Ambrosini and Ferreri, 1998). This allows to solve the problem only in the interval $(0 < s < 1)$, see Fig. 1(b), once the appropriate boundary conditions are specified, in terms of the dimensionless temperature, in $s = 0^+$ and $s = 1^-$. Such boundary conditions are obtained, according to Welander's treatment, by solving the energy equation in the source and in the sink under quasi-steady-state conditions (by virtue of the infinitesimal length of the source and the sink) and assuming an anti-symmetric temperature distribution along the loop. These assumptions lead to the following form for the boundary conditions

$$\theta(0^+, \tau) + \theta(1^-, \tau) = [1 + \theta(1^-, \tau)] \times (1 - e^{-\frac{v}{q^{1-d}}}) \quad \text{for } q > 0, \tau > 0, \quad (12a)$$

$$\theta(0^+, \tau) + \theta(1^-, \tau) = [-1 + \theta(0^+, \tau)] \times (1 - e^{-\frac{v}{|q|^{1-d}}}) \quad \text{for } q < 0, \tau > 0, \quad (12b)$$

where the following dimensionless quantity has been introduced

$$v = \left[\frac{\Pi_w \xi \Delta S}{\rho c_p \bar{Q}^{(1-d)}} \right]^d. \quad (13)$$

Initial conditions are also necessary to determine the unique solution describing the transient evolution of the system; these have the form

$$q(0) = q_0,$$

$$\theta(s, 0) = \theta_0(s) \quad (0 < s < 1).$$

In this paper, initial conditions close to the steady-state ones are chosen and a small perturbation in the flow rate is included.

3. Steady-state conditions

For the thermosyphon loop under investigation, steady-state conditions characterized by negative, zero, or positive flow rate are possible. Due to the symmetry of the loop and of the boundary conditions, we can restrict the analysis, with no loss of generality, to the case of positive flow rate, discarding the less interesting case of zero flow. In fact, as pointed out in Welander (1967) and Ambrosini and Ferreri (1998), the case with negative flow rate is just the mirror image of the one with positive flow.

In the following, \bar{q} and $\bar{\theta}$ are the dimensionless steady-state volumetric flow rate and temperature distribution, respectively.

The momentum equation in the form (9), can be re-written for the steady-state, taking into account that it is $\bar{q} > 0$, as

$$\gamma \bar{q}^2 + \varphi \bar{q}^{2-b} = \alpha \int_0^1 \bar{\theta} ds. \quad (14)$$

The boundary conditions (12), accounting for the symmetry of the problem, produce the following results

$$\theta^+ = \frac{\left(1 - e^{-\frac{v}{\bar{q}^{1-d}}}\right)}{\left(1 + e^{-\frac{v}{\bar{q}^{1-d}}}\right)} \quad \begin{array}{l} \text{(steady-state value of } \theta \text{ along the} \\ \text{ascending leg}), \end{array} \quad (15a)$$

$$\theta^- = -\frac{\left(1 - e^{-\frac{v}{\bar{q}^{1-d}}}\right)}{\left(1 + e^{-\frac{v}{\bar{q}^{1-d}}}\right)} \quad \begin{array}{l} \text{(steady-state value of } \theta \text{ along the} \\ \text{descending leg}). \end{array} \quad (15b)$$

It is now time to spend some words about the procedure used to make the volumetric flow rate dimensionless. Simultaneous consideration of relations (6) and (7c) leads to the equation

$$Q = \frac{\Pi_w \xi \bar{Q}^d \Delta S}{\rho c_p} q, \quad (16)$$

where Q and q are the instantaneous volumetric flow rate and the dimensionless one, respectively. The pretty general relation (16) must obviously hold for the steady-state, giving rise, after proper rearrangements, to

$$\bar{Q} = \left(\frac{\Pi_w \xi \Delta S}{\rho c_p} \bar{q} \right)^{\frac{1}{1-d}}. \quad (17)$$

The above expression represents just the “recipe” to make the volumetric flow rate dimensionless. In order to achieve this result, according to (16), it is therefore necessary to define the dimensionless steady-state volumetric flow rate as in Eq. (17). Since the dimensionless volumetric flow rate is not simply proportional to the actual value, it appears to be a rather unusual procedure. On the other hand, relation (17) is a direct consequence of the attempt to keep the greatest level of similarity with Welander's formalism and, as it appears from relation (16), this choice is not particularly limiting for the developments of the theory.

Relation (17) allows to redefine the dimensionless parameters α , φ , v , all functions of \bar{Q} (which is regarded, up to now, as an assigned value), in the form

$$\varphi = \varphi^* \bar{q}^{\frac{bd}{1-d}}, \quad (18a)$$

$$\alpha = \alpha^* \bar{q}^{\frac{-2d}{1-d}}, \quad (18b)$$

$$v = \bar{q}^{-d}. \quad (18c)$$

Here, the parameters φ^* and α^* depend exclusively on the geometrical and the physical characteristics of the system and do not contain any unknown quantity. In fact, they are defined by the expressions

$$\varphi^* = \frac{a\Pi_w L}{16A^{1-b}} \left[\frac{\mu c_p^{\frac{1}{1-d}}}{\rho^{\frac{-d}{1-d}} D (\Pi_w \xi \Delta S)^{\frac{1}{1-d}}} \right]^b, \quad (19a)$$

$$\alpha^* = \frac{g\beta L \Delta T}{2} \left[\frac{(\rho c_p)^{\frac{1}{1-d}} A}{(\Pi_w \xi \Delta S)^{\frac{1}{1-d}}} \right]^2. \quad (19b)$$

Relations (15) can be rewritten, by virtue of (18c), as

$$\theta^+ = \frac{\left(1 - e^{-\frac{1}{q}}\right)}{\left(1 + e^{-\frac{1}{q}}\right)} \quad \begin{array}{l} \text{(steady-state value of } \theta \text{ along the} \\ \text{ascending leg),} \end{array} \quad (20a)$$

$$\theta^- = - \frac{\left(1 - e^{-\frac{1}{q}}\right)}{\left(1 + e^{-\frac{1}{q}}\right)} \quad \begin{array}{l} \text{(steady-state value of } \theta \text{ along} \\ \text{the descending leg).} \end{array} \quad (20b)$$

Relations (20) can be used to evaluate the integral at the right-hand side of Eq. (14). This leads, after some rearrangements, to the following equation for \bar{q} (steady-state volumetric flow rate)

$$\frac{2 \left[\lambda \bar{q}^{\frac{2}{1-d}} + \sigma \bar{q}^{\frac{(2-b)}{1-d}} \right]}{1 + \left[\lambda \bar{q}^{\frac{2}{1-d}} + \sigma \bar{q}^{\frac{(2-b)}{1-d}} \right]} = \left(1 - e^{-\frac{1}{q}}\right), \quad (21)$$

where the new parameters λ and σ are defined as

$$\lambda = \frac{\gamma}{\alpha^*}, \quad (22a)$$

$$\sigma = \frac{\varphi^*}{\alpha^*}. \quad (22b)$$

It turns out that λ and σ are dependent only on the physical and geometrical features of the loop but not on its length. This means, looking at Eq. (21), that also the dimensionless steady-state flow rate results to be independent of L .

Eq. (21) allows to calculate the volumetric flow rate. It can be easily verified that, when the Darcy friction factor is adopted in place of the Fanning one and when both c and d in (1) and (2) are set equal to zero, the coefficients φ^* and α^* reduce to the dimensionless parameters ε and α used in Ambrosini and Ferreri (1998), respectively. With these assumptions, Eq. (21) for the steady-state reduces to the form there reported.

It is worthwhile to remark that, once the kind of heat transfer correlation (namely the value of d in (2)) has been chosen as well as the coefficients in the friction

factor correlation (1), φ^* and α^* completely determine the steady-state solution of the problem.

4. Stability analysis of the system

The stability of the system can be studied by linearising the momentum and the energy equations as well as the boundary conditions. This technique, also used by Welander, is based on the application of a first-order perturbation method. We assume that the dimensionless volumetric flow rate and temperature can be expressed as the superposition of a steady-state term plus a small perturbation depending on dimensionless time, according to the following expressions

$$q(\tau) = \bar{q} + \delta q(\tau), \quad (23a)$$

$$\theta(s, \tau) = \bar{\theta}(s) + \delta\theta(s, \tau). \quad (23b)$$

As a consequence of (23), the momentum and the energy equations, together with the boundary conditions, reduce to

$$\frac{d(\delta q(\tau))}{d\tau} + \Theta \cdot (\delta q(\tau)) = \alpha \int_0^1 (\delta\theta(s, \tau)) ds, \quad (24a)$$

$$\frac{\partial(\delta\theta(s, \tau))}{\partial\tau} + \bar{q} \frac{\partial(\delta\theta(s, \tau))}{\partial s} = 0, \quad (24b)$$

$$\delta\theta(0^+, \tau) + m \delta\theta(1^-, \tau) + n \delta q(\tau) = 0, \quad (24c)$$

where

$$\Theta = 2\gamma\bar{q} + \varphi(2-b)\bar{q}^{(1-b)}, \quad (25a)$$

$$m = e^{-\frac{1}{q}}, \quad (25b)$$

$$n = 2(1-d) \frac{e^{-\frac{1}{q}}}{\left(1 + e^{-\frac{1}{q}}\right) \bar{q}^2}. \quad (25c)$$

If the time dependence of δq and $\delta\theta$ is assumed to be given by the complex exponential form

$$\delta q(\tau) = \delta q(0) e^{z\tau}, \quad (26a)$$

$$\delta\theta(s, \tau) = \delta\theta(s, 0) e^{z\tau}, \quad (26b)$$

and an integration along the ascending leg ($0 < s < 1$), with the appropriate boundary conditions, is carried out, the following characteristic equation in z is obtained

$$\frac{e^z + m}{e^z - 1} + \frac{\tilde{\alpha}}{z(z + \tilde{\Theta})} = 0, \quad (27)$$

where

$$\tilde{\alpha} = \frac{\alpha n}{\bar{q}}, \quad (28a)$$

$$\tilde{\Theta} = \frac{\Theta}{\bar{q}}. \quad (28b)$$

Table 1

Comparison between theoretical model and numerical results for different combinations of physical and geometrical conditions

Case	a	b	L [m]	$T_{w,\text{source}}$ [°C]	$T_{w,\text{sink}}$ [°C]	ξ [W s ^{0.8} m ^{-4.4} K ⁻¹]	G_{model} [kg/s]/ stable– unstable	G_{code} [kg/s]/ stable– unstable
1	0.316	0.25	5.5	30	20	1078921.9	0.2875/S	0.2777/S
2	0.316	0.25	5.5	30	20	1011489.3	0.2782/U	0.2687/U
3	0.316	0.25	2.5	30	20	876624.1	0.2585/S	0.2444/S
4	0.316	0.25	7.5	30	20	876624.1	0.2585/U	0.2509/U
5	64.0	1.0	60	45	35	636161.7	0.7122/U	0.7170/U
6	64.0	1.0	10	45	35	636161.7	0.7122/S	0.7072/S

Eq. (27) is used to assess the stability of the system. Once the geometric and the physical parameters are assigned, the steady-state volumetric flow rate, as well as the parameters m , $\tilde{\alpha}$ and $\tilde{\Theta}$, can be computed. Eq. (27) can be therefore solved with respect to z to determine the dynamic behaviour of the system: the stable, unstable or neutral conditions are given by $Re(z_1) < 0$, $Re(z_1) > 0$, $Re(z_1) = 0$, respectively, where z_1 is the solution with the largest real part.

It is clear that, once the heat transfer law (2) and the friction factor correlation (1) are defined and all the physical and geometrical parameters are specified, α^* and φ^* completely determine the dynamic behaviour of the system.

5. Numerical experiments and results

A validation of the model has been carried out in comparison with the results of a numerical transient code purposely developed for the one-dimensional analysis of single-phase thermosyphon loops with general enough lay-out (Ambrosini, 2001; Ambrosini et al., 2001). Stability has been assessed by the code on the basis of the observed transient behaviour after a small perturbation of the steady-state conditions.

The main characteristics of the program and of its models are shortly summarised.

- The natural circulation loop is assumed to consist of different sections made of circular pipes having uniform diameter and structure thickness. Each section is axially discretised with uniformly distributed nodes.
- The one-dimensional energy balance equation is solved in the control volumes, by making use of a classical first-order upwind explicit method or, as an alternative, of a low diffusion method devised on the basis of a second order upwind explicit scheme. For better accuracy, the latter numerical scheme has always been adopted in the present work.
- The momentum equation is written for an incompressible fluid in integral form and discretised in time by a semi-implicit technique. The Boussinesq assumption is retained for evaluating buoyancy.

- Walls are thermally coupled with the internal fluid in each node and with appropriate convective boundary conditions on the outer surface. The internal heat transfer coefficient may be calculated by an appropriate constitutive relationship or assigned as an input. In the present application, anyway, heat structures play a minor role as pipes are everywhere considered adiabatic, except in the pointwise heat source and sink.
- A default friction relationship is available in the code. It is anyway possible to specify a user-defined friction law. This possibility has been used in the analysis performed for the present calculation cases.
- Steady-state conditions are evaluated by an algorithm involving two nested iteration loops on the flow rate and the average fluid temperature, with allowance for arbitrary distributions of heating and cooling devices.

The value of the steady-state volumetric flow and the stable or unstable character of the dynamic evolution, as predicted by the two methods (i.e., analytical and numerical), are compared. The heat transfer coefficient in the heat source and in the sink, as well as the friction factor, are chosen to be the same in the analytical model and in the numerical program.

After testing the reliability of the analytical model, the theoretical stability map for a specific example has been compared with the theoretical stability map for the case of constant heat transfer coefficient, the friction factor correlation being the same in the two cases.

5.1. Analytical model validation

The results obtained for some cases of interest are reported in Table 1. For all the cases considered, it has been assumed $c = 0$, $d = 0.8$, $\Delta S = 0.1$ m, $D = 0.1$ m. In Table 2, the characteristics of the nodalisations adopted

Table 2
Nodalisations adopted in numerical calculations for the cases 1–6 of Table 1

Case	Volumes per leg	Volumes in source and sink
1–4	25	1
5–6	50	1

in the numerical code simulations for the different cases are given. The loop flow rate transient evolution calculated using the numerical code in cases 1–6 are shown in Figs. 2–4. Fig. 5 shows the theoretical stability map together with the working points analysed via the nu-

merical code for the specific combinations used in cases 1–4.

The results reported in Table 1 reveal a reasonable agreement between the analytical model and the numerical program as far as the steady-state flow rate and

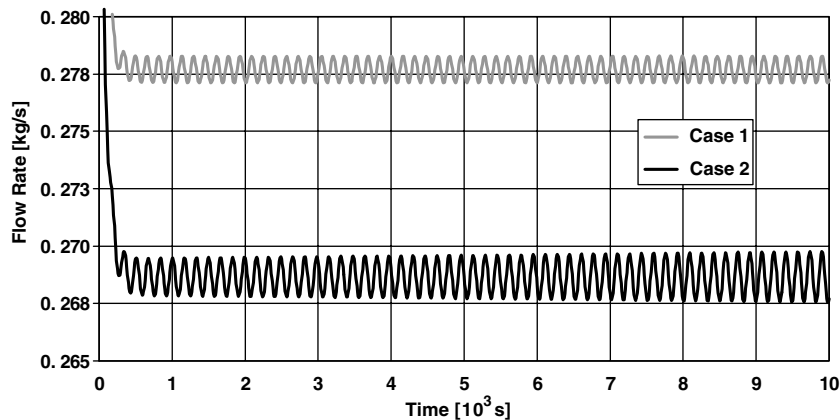


Fig. 2. Loop flow rate transient calculated via the numerical code: case 1 and case 2.

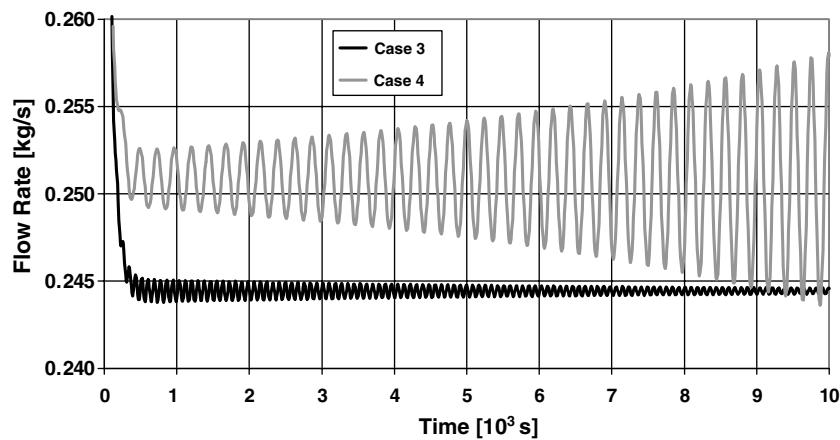


Fig. 3. Loop flow rate transient calculated via the numerical code: case 3 and case 4.

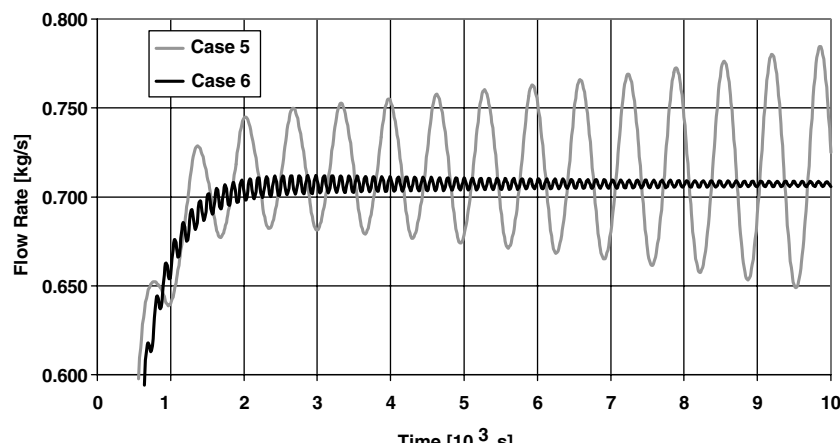


Fig. 4. Loop flow rate transient calculated via the numerical code: case 5 and case 6.

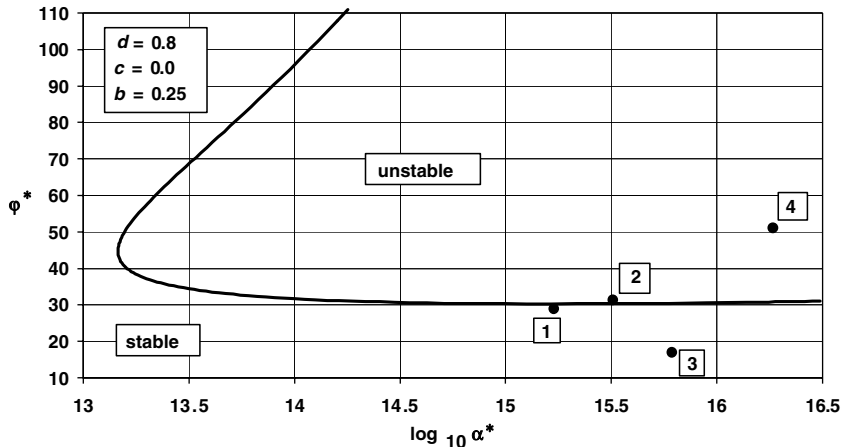


Fig. 5. Theoretical stability map for the positive flow steady-state condition ($d = 0.8$, $c = 0.0$, $b = 0.25$) also showing the location of the considered working points.

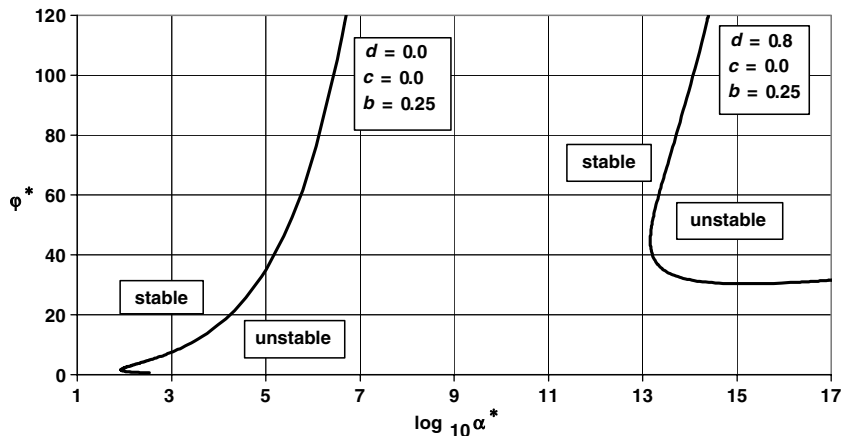


Fig. 6. Comparison of the theoretical stability maps for the cases $d = 0.0$, $c = 0.0$, $b = 0.25$ and $d = 0.8$, $c = 0.0$, $b = 0.25$ (positive flow steady-state conditions).

the assessment of the system stability are concerned, even when the margin of stability or instability is relatively small. The small differences in the steady-state mass flow rate between the analytical model and the reference program can be ascribed to the different nature of the models (analytical and numerical) and to the schematisation of the source and the sink with nodes having finite length.

5.2. Comparison of the stability maps for different heat transfer correlations

The stability map for the case with $d = 0.8$, $b = 0.25$, $c = 0.0$ is reported in Fig. 6 in comparison with the case with $d = 0.0$ (i.e., constant heat transfer coefficient case), $b = 0.25$, $c = 0.0$. The parameter α^* is reported in logarithmic scale along the abscissa. Looking at the representation of the stability map in terms of α^* and φ^* , it

appears from the example that the neutral stability line for the case of variable heat transfer coefficient is displaced in the zone of higher α^* and φ^* values with respect to the case with $d = 0.0$ and has a different appearance, even if it maintains the characteristic "nose" shape.

6. Conclusions

In the present paper, an extension of the analysis proposed by Welander (1967) for a simple single-phase thermosyphon loop is carried out by including more general friction factor and heat transfer coefficient correlations. A five-parameters description of the stability of the system, that is conveniently reduced to a two-parameters representation (namely α^* and φ^*), is demonstrated to be possible and an analytical model is

correspondingly obtained. Such a model has been validated with results provided by a completely independent numerical code incorporating the same friction factor and heat transfer coefficient correlations used in the analytical model in each of the considered cases.

The analytical model has then been used to compare the case of heat transfer coefficient calculated according to a Colburn-type correlation with the case of constant heat transfer coefficient assumed in the original Welander's treatment. This comparison reveals that the neutral stability curve changes in shape and position in the $\alpha^*-\varphi^*$ plane. In particular, for the variable heat transfer coefficient case, the onset of instability occurs at higher values for α^* and φ^* . However, it has to be considered that for assigned physical and geometrical conditions, a change in the form of the heat transfer coefficient (namely of the exponent d) will involve modifications in the values of α^* and φ^* .

Although the presented model is quite general, the heat transfer correlation (2), mainly used in the presence of forced convection, is obviously not able to cover all the cases of practical interest. As known, both friction and heat transfer may be different in natural circulation conditions with respect to forced flow and specific closure laws should be adopted in this case. Further developments, i.e., consideration of other forms of the heat transfer coefficient, would therefore represent the logical step to extend the applicability of the present work. Also the extension to friction factor forms different from (1) could be interesting, as already shown in Ambrosini and Ferreri (2000).

However, in these developments a compromise must be reached between realism and simplicity of the parametric representation. In fact, for practical purposes it is important to attain simple models, anyway able to represent the relevant features of the considered dynamic system. This is what made Welander's problem so relevant for a whole class of natural circulation loops and motivated the extension of its range of application proposed in the present work.

Acknowledgements

The first two authors would like to acknowledge the EU for supporting the research. Part of this work has been financed by the EU 5th framework programme project NACUSP.

References

Ambrosini, W., 2001. On some physical and numerical aspects in computational modelling of one-dimensional flow dynamics. In: 7th International Seminar on Recent Advances in Fluid Mechanics, Physics of Fluids and Associated Complex Systems (Fluidos 2001), Buenos Aires, Argentina, October 17–19, 2001.

Ambrosini, W., Ferreri, J.C., 1998. The effect of truncation error on the numerical prediction of linear stability boundaries in a natural circulation single-phase loop. *Nucl. Eng. Des.* 183, 53–76.

Ambrosini, W., Ferreri, J.C., 2000. Stability analysis of single-phase thermosyphon loops by finite-difference numerical methods. *Nucl. Eng. Des.* 201, 11–23.

Ambrosini, W., D'Auria, F., Pennati, A., Ferreri, J.C., 2001. Numerical effects in the prediction of single-phase natural circulation stability. In: National Heat Transfer Conference of UIT, Modena, Italy, June 25–27.

Bau, H.H., Torrance, K.E., 1981. Transient and steady behaviour of an open, symmetrically heated, free convection loop. *Int. J. Heat Mass Transfer* 24, 597–609.

Bau, H.H., Wang, Y.Z., 1992. Chaos: a heat transfer perspective. In: Tien, L. (Ed.), *Annual Review of Heat Transfer*, vol. 4. Hemisphere Publishing Co.

Challberg, R.C., Cheung, Y.K., Khorana, S.S., Upton, H.A., 1998. ESBWR evolution of passive features. In: 6th International Conference on Nuclear Engineering (ICON-6), San Diego, USA, May 10–15, 1998.

Chen, K., 1985. On the oscillatory instability of closed loop thermosyphons. *J. Heat Transfer, Trans. ASME* 107 (November), 826–832.

Creveling, H.F., De Paz, J.F., Baladi, J.Y., Schoenals, R.J., 1975. Stability characteristics of a single-phase free convection loop. *J. Fluid Mech.* 67, Part 1, 65–84.

Frogheri, M., Misale, M., D'Auria, F., 1997. Experiments in single-phase natural circulation. In: 15th UIT National Heat Transfer Conference 1997, Torino, June 19–20, 1997.

Greif, R., Zvirin, Y., Mertol, A., 1979. The transient and stability behaviour of a natural convection loop. *J. Heat Transfer, Trans. ASME* 101 (November), 684–688.

Hart, J.E., 1984. A new analysis of the closed loop thermosyphon. *Int. J. Heat Mass Transfer* 27 (1), 125–136.

Hart, J.E., 1985. A note on the loop thermosyphon with mixed boundary conditions. *Int. J. Heat Mass Transfer* 28 (5), 939–947.

Hilborn, R.C., 2000. *Chaos and Nonlinear Dynamics, An Introduction for Scientists and Engineers*, second ed. Oxford University Press.

Keller, J.B., 1966. Periodic oscillations in a model of thermal convection. *J. Fluid Mech.* 26, Part 3, 599–606.

Lorenz, E.N., 1963. Deterministic non-periodic flow. *J. Atmos. Sci.* 20, 130–141.

Misale, M., Tagliafico, L., 1987. The transient and stability behaviour of single-phase natural circulation loops. *Heat Technol.* 5 (1–2).

Misale, M., Frogheri, M., D'Auria, F., 1999. Experiments in natural circulation: influence of scale factor on the stability behavior. In: Eurotherm Seminar No. 63 on Single and Two-Phase Natural Circulation, September 6–8, 1999, Genoa, Italy.

Rodriguez-Bernal, A., 1995. Attractors and inertial manifolds for the dynamics of a closed thermosyphon. *J. Math. Anal. Appl.* 193, 942–965.

Sen, M., Ramos, E., Treviño, C., 1985. The toroidal thermosyphon with known heat flux. *Int. J. Heat Mass Transfer* 28 (1), 219–233.

Velazquez, J.J., 1994. On the dynamics of a closed thermosyphon. *SIAM J. Appl. Math.* 54 (December), 1561–1593.

Venkat Raj, V., 1994. Experimental studies related to thermosyphon cooling of nuclear reactors—a review. In: Proceedings of the First ISHMT-ASME Heat and Mass Transfer Conference and Twelfth National Heat and Mass Transfer Conference, January 5–7, 1994, Bhabha Atomic Research Centre, Bombay, India.

Vijayan, P.K., 2002. Experimental observations on the general trends of the steady state and stability behaviour of single-phase natural circulation loops. *Nucl. Eng. Des.* 215 (1–2), 139–152.

Vijayan, P.K., Austregesilo, H., 1994. Scaling laws for single-phase natural circulation loops. *Nucl. Eng. Des.* 155, 331–347.

Vijayan, P.K., Date, A.W., 1990. Experimental and theoretical investigations on the steady-state and transient behaviour of a

thermosyphon with throughflow in a figure-of-eight loop. *Int. J. Heat Mass Transfer* 33 (11), 2479–2489.

Vijayan, P.K., Date, A.W., 1992. The limits of conditional stability for single-phase natural circulation with throughflow in a figure-of-eight loop. *Nucl. Eng. Des.* 136, 361–380.

Vijayan, P.K., Austregesilo, H., Teschendorff, V., 1995. Simulation of the unstable behavior of single-phase natural circulation with repetitive flow reversals in a rectangular loop using the computer code ATHLET. *Nucl. Eng. Des.* 155, 623–641.

Welander, P., 1965. Steady and oscillatory motions of a differentially heated fluid loop. Woods Hole Oceanographic Institute, Ref. No. 65-48 (unpublished manuscript).

Welander, P., 1967. On the oscillatory instability of a differentially heated fluid loop. *J. Fluid Mech.* 29, Part 1, 17–30.

Zvirin, Y., 1979. The effect of dissipation on free convection loops. *Int. J. Heat Mass Transfer* 22, 1539–1545.

Zvirin, Y., Greif, R., 1979. Transient behaviour of natural circulation loops: two vertical branches with point heat source and sink. *Int. J. Heat Mass Transfer* 22, 499–504.